# Patterns of grey and white matter changes differ between bulbar and limb onset amyotrophic lateral sclerosis

Robert Steinbach [a],[*],[1], Tino Prell [a],[b], Nayana Gaur [a], Annekathrin Roediger [a], Christian Gaser [a],[b],[c], Thomas E. Mayer [d], Otto W. Witte [a],[b], Julian Grosskreutz [a],[b]

[a] Hans Berger Department of Neurology, Jena University Hospital, Jena, Germany
[b] Center for Healthy Ageing, Jena University Hospital, Jena
[c] Department of Psychiatry and Psychotherapy, Jena University Hospital, Jena, Germany
[d] Department of Neuroradiology, Jena University Hospital, Jena, Germany

A R T I C L E   I N F O

A B S T R A C T

Amyotrophic Lateral Sclerosis (ALS) is a progressive neurodegenerative disease that is characterized by a high heterogeneity in patients' disease course. Patients with bulbar onset of symptoms (b-ALS) have a poorer prognosis than patients with limb onset (l-ALS). However, neuroimaging correlates of the assumed biological difference between b-ALS and l-ALS may have been obfuscated by patients' diversity in the disease course. We conducted Voxel-Based-Morphometry (VBM) and Tract-Based-Spatial-Statistics (TBSS) in a group of 76 ALS patients without clinically relevant cognitive deficits. The subgroups of 26 b-ALS and 52 l-ALS patients did not differ in terms of disease Phase or disease aggressiveness according to the D50 progression model. VBM analyses showed widespread ALS-related changes in grey and white matter, that were more pronounced for b-ALS. TBSS analyses revealed that b-ALS was predominantly characterized by frontal fractional anisotropy decreases. This demonstrates a higher degree of neurodegenerative burden for the group of b-ALS patients in comparison to l-ALS. Correspondingly, higher bulbar symptom burden was associated with right-temporal and inferior-frontal grey matter density decreases as well as fractional anisotropy decreases in inter-hemispheric and long association tracts. Contrasts between patients in Phase I and Phase II further revealed that b-ALS was characterized by an early cortical pathology and showed a spread only outside primary motor regions to frontal and temporal areas. In contrast, l-ALS showed ongoing structural integrity loss within primary motor-regions until Phase II. We therefore provide a strong rationale to treat both onset types of disease separately in ALS studies.

## 1. Introduction

Amyotrophic Lateral Sclerosis (ALS) is a fatal, progressive neurodegenerative disease. The clinical course of ALS is highly heterogeneous, especially in terms of the first affected body region, the sequential spread to other regions, and the progression of the disease. The uncertainty in predicting the awaited individual progress, in particular for newly diagnosed patients, hampers adequate therapeutic management and challenges research in ALS (Simon et al., 2014; Westeneng et al., 2018). Patients with bulbar onset of symptoms (b-ALS) have a poorer prognosis than patients with limb onset (l-ALS) (Calvo et al., 2017; Ganesalingam et al., 2009; Trojsi et al., 2017). However, it remains unclear, if the shorter survival time in b-ALS is caused by bulbar complications (i.e., aspiration-pneumonia), or if b-ALS represents a biologically different entity with a higher degree of pathological progressivity. If b-ALS and l-ALS are biologically divergent, one would expect different

patterns of neurodegeneration which should be detectable with means of neuroimaging.

Previous cerebral Magnetic Resonance Imaging (MRI) studies have demonstrated their potential to reveal ALS-related structural alterations of neuronal integrity on a case-control-level (Alruwaili et al., 2018; Floeter et al., 2018; Zhang et al., 2018, 2017). However, neuroimaging studies attempting to demonstrate direct differences between b-ALS and l-ALS have shown either no or conflicting results (Bede et al., 2013; Borsodi et al., 2017; Cardenas-Blanco et al., 2014; Hartung et al., 2014; Kim et al., 2017; Prell et al., 2013; van der Graaff et al., 2011). These inconsistencies may result from different methodology but also incomplete characterization and deficient matching of the ALS subgroups. Moreover, if an onset of ALS with bulbar symptoms causes a higher degree of neurodegeneration, one might expect a correlation between the severity of bulbar dysfunction and neuroimaging signals. Again, such associations have been inconsistently reported or not found (Roccatagliata et al., 2009; Shellikeri et al., 2019). This problem has been addressed in a wider context as the 'correlation gap', that typically occurs in ALS neuroimaging studies (Verstraete et al., 2015).

We therefore aimed to explore the neuroimaging patterns in b-ALS and l-ALS in a large cohort of well-characterized patients with normal cognitive performance. To take the high heterogeneity of patients' individual disease course into account we applied the D50 progression model which provides distinct measures of disease aggressiveness and individual disease covered (Poesen et al., 2017; Prell et al., 2020; Steinbach et al., 2020a, 2021). We hypothesized that this approach might overcome former obstacles of cross-sectional and longitudinal studies and thus help to unravel the neuroimaging correlates of the neurodegenerative burden in b-ALS.

## 2. Material and methods

### 2.1. Subject identification and clinical characterization

All participants were consecutively recruited from the Department of Neurology at Jena University Hospital in the time period from May 2009 until December 2018. Written informed consent was obtained from individual participants prior to study commencement. All experimental procedures conducted for this study were approved by the local Ethics committee (Nr 3633–11/12) and were in accordance with the ethical standards defined in the 1964 Declaration of Helsinki and its later amendments.

Disease severity was assessed with the revised ALS Functional Rating Scale (ALSFRS-R) (Cedarbaum et al., 1999). For patients with ALS, the D50 model was applied to characterize the individual clinical disease course (Poesen et al., 2017; Prell et al., 2020; Steinbach et al., 2020a, 2021), which is modelled based on all available ALSFRS-R scores. The derived D50 value depicts the overall disease aggressiveness, defined as the estimated time taken in months for a patient to lose 50% of his/her functionality. The relative D50 (rD50) is calculated through normalization of patients' real-time disease trajectories to D50 and depicts the individual disease covered, independent of aggressiveness. Thus, rD50 allows the comparability of patients with vastly differing disease aggressiveness and constitutes an open-ended reference point with 0 = disease onset and 0.5 = time-point of halved functionality. Based on the rD50, patients can be categorized into at least 3 Phases: an early semi-stable Phase I ($0 \leq$ rD50 $< 0.25$), an early progressive Phase II ($0.25 \leq$ rD50 $< 0.5$), and late progressive and late stable Phases III/IV (rD50 $\geq 0.5$). In addition, based on the calculated disease curve, measures of local disease activity can be calculated for any time-point (here at MRI), namely the calculated functional state and the calculated functional loss rate. In order to select patients with high reliability in the D50 modelling and moderate variability for the resulting parameters, we only included patients who received at least two ALSFRS-R scorings during their disease course and had a D50 value below 100 months (Steinbach et al., 2020b).

Inclusion criteria were: the patients with ALS were able to perform MRI investigation and eventually met the revised El-Escorial-criteria of definite, probable or laboratory-supported probable ALS (Brooks et al., 2000). Exclusion criteria were: juvenile ALS, primary lateral sclerosis, manifest dementia or other comorbidities that could affect motor performances. We also excluded patients with cognitive deficits or unavailable/incomplete cognitive testing according to neuropsychological screening assessments: For patients enrolled before 2015 these were Mini-Mental State Examination $< 26$ points (Creavin et al., 2016) and/or frontal assessment battery $< 13.5$ points (Appollonio et al., 2005; Dubois et al., 2000). For patients enrolled after 2015 the Edinburgh Cognitive and Behavioural Amyotrophic Lateral Sclerosis Screen (ECAS) was used with German education and age-adjusted cutoffs (Abrahams et al., 2014; Lule et al., 2015).

We only included patients who had received ALSFRS-R scoring within 10 days prior to or after MRI, in order to calculate more traditionally used disease metrics for comparison purposes. The Progression Rate is calculated as linearly averaged loss of ALSFRS-R points per month since symptom onset ((48-ALSFRS)/symptom duration). The King's Staging system allocates patients to Stages I (involvement of one clinical region) through IV (respiratory or nutritional failure), whilst the MiToS System describes Stages 0 (functional involvement) through IV (loss of independence in four domains), the Stages V depict patients' death for both staging systems respectively (Chio et al., 2015; Roche et al., 2012).

Lastly, 78 ALS patients and 69 healthy control participants were included in the study cohort for neuroimaging analyses (for a CONSORT diagram please refer to Supplementary Figure S1).

### 2.2. MRI data acquisition and processing

All MRI images were obtained according to a harmonized protocol at the same 1.5 Tesla Siemens Sonata scanner.

The T1-weighted images were acquired in a FLASH 3D sequence (repetition time $= 15$ ms, echo time $= 5$ ms, Flip Angle $= 30°$, slice thickness 1 mm, pixel size 1 mm $\times$ 1 mm, acquisition matrix $256 \times 240$). Image processing was conducted as before, using the pipeline of the CAT12-toolbox (version 1450, http://www.neuro.uni-jena.de/cat/) for standardized Voxel-Based Morphometry (VBM) analyses (Steinbach et al., 2020a). The Total intracranial Volume (TIV) was calculated as implemented in the CAT12 toolbox and was used as nuisance co-variate for all VBM analyses.

For the Diffusion-Tensor-Images (DTI), 30 diffusion-weighted images (at b $= 1000$ s/mm$^2$) and 3 b $= 0$ images were acquired in a gradient-weighted spin-echo sequence using the following parameters: repetition time 7800 ms, echo time 97 ms, flip angle 90°, slice thickness 2.5 mm, pixel size 1.25 mm $\times$ 1.25 mm, acquisition matrix $96 \times 96$. The standardized pipeline for Tract–Based Spatial Statistics (TBSS) was applied using the FRMRIB Software Library (FSL, version 5.0) and resulted in normalized and skeletonized maps of Fractional Anisotropy (FA), Mean Diffusivity (MD), Axial Diffusivity (AD) and Radial Diffusivity (RD) (see also Steinbach et al. (2021)).

Upon dual inspection of structural MRI datasets (FLAIR and T1 weighted, done by RS and TM), subjects with intracranial pathologies that could affect the analyses (such as tumors, cysts, stroke or bleedings) were excluded. Representative images that resulted after processing (FA and T1 segments) were again visually inspected (by RS) and sorted out if any image artefacts/processing failures were observed.

For illustration purposes, we marked the mototopic regions of the primary motor cortex (PMC). These had been used from the Brainnetome Atlas (http://atlas.brainnetome.org), as parcellations of Brodmann's Area 4 representing a) tongue and larynx, b) head and face, c) upper limbs, d) trunk and e) lower limbs (Fan et al., 2016; Genon et al., 2018).

**Table 1**

Demographic and Clinical Data for patients with bulbar-onset and limb-onset Amyotrophic Lateral Sclerosis.

| ALS (n = 78) | bulbar (b-ALS) | | | limb (l-ALS) | | | p |
|---|---|---|---|---|---|---|---|
| *Demographics* | | | | | | | |
| n | 26 | | | 52 | | | - |
| age [years] *$* | 71.04 ± 14.7 | | | 63.45 ± 15.0 | | | 0.016* |
| | (64.33–74.0) | | | (59.75–65.5) | | | |
| gender [male/female] *#* | 9/17 | | | 37/15 | | | 0.002* |
| | 34.6%/65.4% | | | 71.2%/28.8% | | | |
| handedness [left/right] *#* | 1/25 | | | 5/47 | | | 0.342 |
| | 3.8%/96.2% | | | 9.6%/90.4% | | | |
| *neurocognitive screening* | | | | | | | |
| ECAS [points] *$* | *for n = 17:* | | | *for n = 32:* | | | *n = 49:* |
| ECAS total score | 164 ± 38.0 (148–176) | | | 155 ± 32.0 (150–162) | | | 0.244 |
| ALS-specific subscore | 79.0 ± 19.0 (74–87) | | | 74.5 ± 15.0 (72–78) | | | 0.275 |
| Non-ALS-specific subscore | 85.0 ± 19.0 (76–89) | | | 79.0 ± 16.0 (78 – 84) | | | 0.270 |
| FAB [points] *$* | *for n = 9:* | | | *for n = 20:* | | | *n = 29:* |
| | 18.0 ± 0.5 (18–18) | | | 18.0 ± 1.8 (18–18) | | | 0.255 |
| MMSE [points] *$* | *for n = 9:* | | | *for n = 20:* | | | *n = 29:* |
| | 30.0 ± 1.0 (30–30) | | | 29.0 ± 1.0 (29–30) | | | 0.337 |
| *traditional disease metrics* | | | | | | | |
| ALSFRS-R total score [points] *$* | 40.0 ± 9.0 (38–43) | | | 39.0 ± 10.5 (37–42) | | | 0.738 |
| ALSFRS-R bulbar subscore | 7.0 ± 4.0 (7–9) | | | 11.0 ± 2.0 (11–12) | | | <0.001* |
| ALSFRS-R fine-motor subsc. | 11.0 ± 3.0 (10–12) | | | 9.0 ± 4.0 (9–10) | | | <0.001* |
| ALSFRS-R gross-motor subsc. | 11.5 ± 3.0 (10–12) | | | 8.5 ± 6.0 (7–10) | | | 0.002* |
| ALSFRS-R ventilatory subsc. | 12.0 ± 1.0 (12–12) | | | 12.0 ± 1.0 (12–12) | | | 0.506 |
| symptom duration [months] *$* | 12.5 ± 9.0 | | | 13.5 ± 15.0 | | | 0.348 |
| | (9.0–16.0) | | | (11.0–18.0) | | | |
| progression rate [points lost per month] *$* | 0.63 ± 0.5 | | | 0.5 ± 0.5 | | | 0.542 |
| | (0.43–0.8) | | | (0.4–0.77) | | | |
| King's stage *#* | I: | 10 | 38.5% | I: | 14 | 26.9% | 0.721 |
| | II: | 9 | 34.6% | II: | 15 | 28.8% 34.6% | |
| | III | 6 | 23.1% | III | 18 | 1.9% | |
| | IVa: | 0 | 0% | IVa: | 1 | 7.7% | |
| | IVb: | 1 | 3.8% | IVb: | 4 | 0% | |
| | V: | 0 | 0% | V: | 0 | | |
| MiToS stage *#* | 0: | 24 | 92.3% | 0: | 40 | 76.9% | 0.243 |
| | I: | 2 | 7.7% | I: | 11 | 12.1% 1.9% | |
| | II: | 0 | 0% | II: | 1 | 0% | |
| | III-V: | 0 | 0% | III-V: | 0 | | |
| *D50 disease progression model parameters* | | | | | | | |
| D50 [months] *$* | 23.98 ± 13.04 | | | 31.97 ± 19.16 | | | 0.105 |
| | (22.07–28.76) | | | (29.57–35.51) | | | |
| relative D50 (rD50) *§* | 0.26 ± 0.1 | | | 0.26 ± 0.1 | | | 0.925 |
| | (0.21–0.31) | | | (0.23–0.30) | | | |
| Phase I (0 ≤ rD50 < 0.25) *#* | I: | 11 | 42.3% | I: | 24 | 46.2% | 0.913 |
| Phase II (0.25 ≤ rD50 < 0.5) | II: | 14 | 53.8% | II: | 26 | 50.0% | |
| Phase III/IV (rD50 ≥ 0.5) | III/IV: | 1 | 3.8% | III/IV: | 2 | 3.8% | |
| calculated functional state [points] *§* | 38.77 ± 5.9 | | | 38.37 ± 6.6 | | | 0.793 |
| | (36.41–41.14) | | | (36.52–40.21) | | | |
| calculated functional loss rate [points lost per month] *$* | 0.85 ± 0.7 | | | 0.74 ± 0.7 | | | 0.194 |
| | (0.67–1.25) | | | (0.54–0.88) | | | |

Continuous data is summarized for *§* as mean ± standard deviation or for *$* as median ± interquartile range (each with the 95% confidence interval of the median in brackets). For categorial data (*#*), the number of cases and percentages are given. For comparison purposes, the Progression Rate, classifications according to the King's Staging system or the MiToS System are given, each calculated from the ALSFRS-R score at MRI.

*Abbreviations: ALS* Amyotrophic Lateral Sclerosis*; ALSFRS-R* revised ALS Functional Rating Scale, with bulbar subscore-sums of items 1–3, with fine-motor subscore-sums of items 4–6, with gross-motor subscore-sums of items 7–9 and with ventilatory subscore-sums of items 10–12; *b-ALS* bulbar-onset ALS; *D50* estimated time in months for an individual to lose 50% of functionality; *l-ALS* limb-onset ALS; *MRI* Magnetic Resonance Imaging.

### 2.3. Statistical analyses

All statistical analyses were performed using the SPSS® software program (IBM®, v26.0.0.0). Non-normal distribution of all demographic and clinical variables was established using the Shapiro Wilks test. Metric variables are expressed as mean with standard deviation, skewed variables as median with interquartile-range and categorical variables as number and percentage. Comparison of group-wise means for demographic and clinical variables were appropriately conducted either with a two-sample *t*-test, a Mann-Whitney-*U* test, or chi-square-/ Fisher-exact test.

A voxel-wise general linear model was applied on the VBM as well as TBSS maps, using permutation-based nonparametric testing with a threshold-free cluster enhancement (TFCE) method, as implemented in FSL for the TBSS analyses (Winkler et al., 2014) and using the TFCE toolbox (version 1.0 r186, http://dbm.neuro.uni-jena.de/tfce/) for the VBM analyses (Smith and Nichols, 2009; Winkler et al., 2014). All inter-group comparisons have been corrected for age and gender as possibly confounding co-variates and all VBM analyses have been additionally corrected for TIV as recommended.

We applied ANOVA designs with additional covariates for inter-group comparisons. On a case-control-level, we compared patients with bulbar onset (b-ALS) with healthy controls as well as patients with limb onset (l-ALS) versus controls. The resulting statistical maps were Family-Wise Error (FWE) corrected to account for multiple comparisons. A strict significance level of a *p*-value below 0.001 was applied for case-

control contrasts, according to our former results (Steinbach et al., 2020a).

In addition, we conducted direct subgroup comparisons between the b-ALS and l-ALS group. To further examine the temporal evolution of changes, additional contrasts of patients in Phase I versus those in Phase II were conducted, separately for the b-ALS and l-ALS group. Here, a $p$-value below 0.05 with FWE-correction was applied for all subgroup analyses.

Additional regression designs were applied to search for possible correlations with the total ALSFRS-R as well as with the bulbar subscore (ALSFRS-R items 1–3), with the fine (ALSFRS-R items 4–6) and with the gross motor functions subscore (ALSFRS-R items 4–9). For the regression analyses, a significance level of an FWE-corrected $p$-value below 0.05 was applied, that was additionally Bonferroni-corrected to account for the numerous regression tests (resulting $p$-values for VBM were 0.005 and for TBSS 0.0025).

## 3. Results

### 3.1. Study cohort

Both cohorts, ALS and controls, had an equal gender distribution with 41 females in the ALS group (41.0%) and 37 female controls (53.6%; $p = 0.127$). However, patients with ALS were older than healthy controls (ALS: median 64.8 years, IQR 17.6; controls: median 53.7 years, IQR 14.2; $p < 0.001$).

In the ALS cohort, 26 had bulbar and 52 limb onset of symptoms. Comparative clinical and demographic data is presented in Table 1. Notably, the b-ALS patients were older and included more women than the l-ALS patients. Consequently, these (age and gender) were included as nuisance covariates in all inter-group analyses. The b-ALS and l-ALS did not significantly differ in terms of D50 model parameters characterizing disease covered (rD50, Phase, calculated functional state) nor the overall or acute disease aggressiveness (D50, calculated functional loss rate; see also Supplementary Fig. S2).

### 3.2. VBM group results

In comparison to healthy controls, patients with b-ALS and l-ALS showed widespread decrease of GM density in bilateral frontal, parietal, temporal and occipital lobes and in the upper hemispheres of the cerebellum ($p < 0.001$, FWE corrected, Fig. 1A&B). The subgroup comparison between l-ALS and b-ALS revealed for b-ALS density decreases, also located in bilateral frontal, parietal, temporal and occipital lobes. According to the general motoric organization (homunculus) of the primary motor cortex (PMC), density decreases of b-ALS versus l-ALS were most evident within regions representing orofacial body parts (emphasized for the right site), distal parts of the lower limbs and to a lesser extend also upper-limb regions ($p < 0.05$, FWE corrected, Fig. 1C).

The WM contrasts showed also decreased density within the associated fiber tracts of the bifrontal, bitemporal and biparietal lobes, either for b-ALS or for l-ALS in the respective case-control-comparisons ($p < 0.001$, FWE corrected, Fig. 1A&B). In comparison to l-ALS, the b-ALS subgroup showed WM density decreases in bilateral frontal, medial-temporal and to a minor extend parietal WM, all as a tendency more emphasized for the right hemisphere. Within the PMC, WM density decreases could be shown underlying the orofacial and neighboring upper-limb representation regions, again most evident for the right hemisphere ($p < 0.05$, FWE corrected, Fig. 1C).

For an overview of all VBM group results readers are also referred to Supplementary Table S1. No GM or WM density increases could be revealed, neither for b-ALS versus l-ALS, nor for b-ALS/l-ALS relative to the control group ($p < 0.05$, FWE corrected).

### 3.3. TBSS group results

In comparison to healthy controls, the patients with b-ALS showed decreased FA-values within pathways of both frontal and temporal lobes, all more emphasized for the right hemisphere ($p < 0.001$, FWE corrected, Fig. 2A). The main affected pathways shown in this contrast encompassed the body of the corpus callosum and adjacent corona radiata, both superior and inferior longitudinal fasciculi and the right-hemispheric inferior fronto-occipital fasciculus, the right uncinate fasciculus as well as parts of bihemispheric external and internal capsules. In comparison to healthy controls, the b-ALS patients showed increased RD values within pathways that were mainly co-localized with the decreased FA values ($p < 0.001$, FWE corrected, Fig. 2B). The MD changes for the comparison of b-ALS and controls were more restricted and localized in the body and genu of the Corpus Callosum ($p < 0.001$, FWE corrected, Fig. 2C).

In comparison to healthy controls, l-ALS patients did only show a small cluster of decreased FA, located subcortical of the right precentral gyrus ($p < 0.001$, FWE corrected Fig. 2D). Increased RD was found within smaller parts of bifrontal white matter and in addition within subcortical parts of both CSTs ($p < 0.001$, FWE corrected, Fig. 2E). The most significant changes for the comparison of l-ALS and healthy controls were observed for increased MD, localized again mainly in bifrontal WM, including both CSTs reaching down until the mesencephalon ($p < 0.001$, FWE corrected, Fig. 2F).

The direct comparison between l-ALS and b-ALS patients revealed only significant differences for the FA contrast in right-hemispheric pathways and none for MD or RD. Here, b-ALS patients showed relatively decreased FA localized within the right fronto-occipital fasciculus, the Forceps Minor, the external capsule and the uncinate fasciculus ($p < 0.05$, FWE corrected, Fig. 2G).

For an overview of all TBSS group results readers are also referred to Supplementary Table S2. None of the mentioned subgroup comparisons showed any statistically significant changes in AD (increases or decreases), FA increases, MD decreases or RD decreases.

### 3.4. Structural changes across the relative disease course

For b-ALS patients in Phase II compared to those in Phase I, the VBM analyses revealed GM density decreases of bilateral temporal and inferio-frontal lobes. The WM VBM showed corresponding density decreases mainly in subcortical regions adjacent to the cortical changes ($p < 0.05$, FWE corrected, Fig. 4A). Notably, the PMC region was totally spared in the GM as well as the WM contrasts, except a small portion of the left-hemispheric tongue/larynx region.

For l-ALS, the comparison of patients in Phase II compared to those in Phase I revealed also cortical and subcortical density decreases in frontal and temporal regions for GM and WM respectively, and within both thalami ($p < 0.05$, FWE corrected, Fig. 4B). However, these presented less extensive than the changes observed for b-ALS patients. Importantly, the l-ALS patients showed relevant changes within the PMC over the disease course, localized mainly in the left hemispheric motoric areas representing the upper limbs.

For TBSS analyses, there were no significant changes in FA, MD, RD or AD in Phase II relative to Phase I patients, neither for the b-ALS nor for the l-ALS group, as reported earlier (Steinbach et al., 2021).

### 3.5. Voxel-wise regression analyses with clinical parameters

We tested for correlations of the ALSFRS-R total as well as sub-scores with structural MRI parameters of VBM and TBSS in regression analyses (Fig. 4).

Widespread negative correlation for RD and mainly co-localized for MD have been found with the total ALSFRS-R score, whilst positive correlations for the FA contrast have been more restricted ($p < 0.0025$, FWE corrected, Fig. 4A-C). For the latter, parts of the body of the corpus
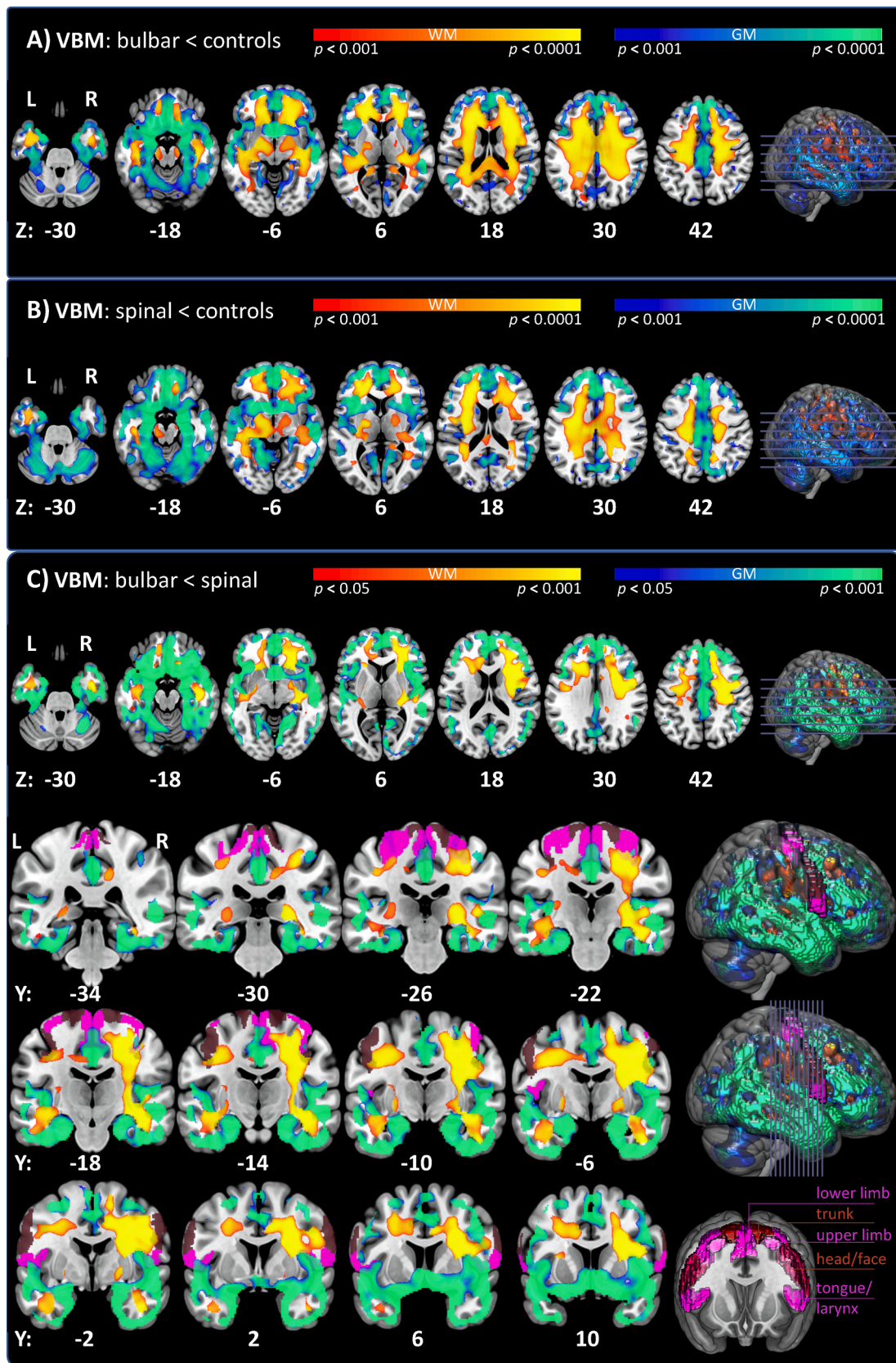
*(caption on next page)*

**Fig. 1.** VBM group analyses of bulbar versus limb-onset ALS. The pictures show *p*-thresholded contrasts of VBM inter-group comparisons of GM (blue-green colorbar) and WM (red-yellow colorbar) overlaid on the MNI152_2009 template of MRIcroGL. Additionaly, regions of the motopopic organization of the PMC have been overlaid (derived from the Brainnetome Atlas, in violet and brown colors). A) B-ALS vs. healthy controls: GM VBM showed decreased density for b-ALS within bilateral frontal, temporal, parietal and occipital lobes as well as parts of the cerebellum. The WM contrasts showed also decreased density within associated fiber tracts of the bifrontal, bitemporal and biparietal lobes (TFCE; FWE corrected *p* < 0.001; nuisance co-variates: age, gender, TIV). B) L-ALS vs. healthy controls: GM as well as WM VBM showed density decreases within the same regions as for b-ALS vs. healthy controls, although as a tendency less widespread (TFCE; FWE corrected *p* < 0.001; nuisance co-variates: age, gender, TIV). C) B-ALS vs. l-ALS: b-ALS showed more density decreases in bilateral frontal, parietal, temporal and occipital lobes as well as WM decreases in bilateral frontal, medial-temporal and to a minor extend parietal WM. Within the PMC, GM regions representing orofacial body parts and distal parts of the lower limbs showed lower densities for b-ALS. For WM, such density decreases underlay orofacial and neighboring upper-limb representation regions of the PMC, all again more emphasized for the right site. (TFCE; FWE corrected *p* < 0.05; nuisance co-variates: age, gender, TIV). *Abbreviations: ALS:* Amyotrophic Lateral Sclerosis; *b-ALS:* bulbar-onset ALS; *FWE:* Family-Wise Error; *GM:* Grey Matter; *l-ALS:* limb-onset ALS; *PMC:* Primary Motor Cortex; *TFCE:* Threshold-Free Cluster Enhancement; *TIV:* Total Intracranial Volume; *WM:* White Matter. (For interpretation of the references to colour in this figure legend, the reader is referred to the web version of this article.)

callosum and adjacent corona radiata showed a positive correlation of FA with the total ALSFRS-R. Negative correlations for AD did not exceed the threshold of the Bonferroni-corrected *p*-value.

A positive correlation with the bulbar-subscore of the ALSFRS-R was also revealed for FA in the TBSS analyses (*p* < 0.0025, FWE corrected, Fig. 4D). These were localized within the entire corpus callosum with corona radiata and in addition long association tracts such as the inferior and superior longitudinal fasciculi, the occipito-frontal fasciculi, uncinate fasciculi as well as the CSTs. Negative correlations of the bulbar subscore with the RD were restricted to body and genu of the Corpus callosum (*p* < 0.0025, FWE corrected, Fig. 4E). Negative correlations for AD or MD did not exceed the threshold of the Bonferroni-corrected *p*-value.

No TBSS regression analyses revealed any significant correlations with either the fine-, gross- or ventilatory-subscore (also not for *p*-values of 0.05 before Bonferroni adjustment).

For the VBM GM analyses, a positive correlation was revealed with the bulbar subscore, indicating density decreases that were associated with increased bulbar symptom burden (*p* < 0.005, FWE corrected, Fig. 4F). These were localized in the inferior frontal gyrus and in the right temporal lobe, including the medial, superior gyrus, the temporal pole as well as the medial temporal lobe and the Amygdala. All other GM as well as WM VBM regression analyses did not reveal any significant correlations, neither for any of the ALSFRS-R sub-scores nor for the total score. Applying the original *p*-values of 0.05 would only reveal a positive correlation of the total score with GM, mirroring parts of the contrast that showed a correlation with the bulbar subscore.

## 4. Discussion

This study compared MRI measures of cerebral structural integrity between cognitively normal b-ALS and l-ALS, whilst carefully considering patient's individual disease course. We evaluated, that both subgroups did not differ in terms of disease covered/Phase or disease aggressiveness, using the D50 model. With means of VBM we could show, that the widespread ALS-related changes in GM and WM including all cerebral lobes, were more pronounced for b-ALS (Fig. 1). The TBSS analyses revealed changes in corresponding WM regions, where b-ALS was predominantly characterized through frontal FA decreases (Fig. 2). The pseudo-longitudinal comparisons of patients in disease Phase I versus Phase II revealed a differentiated pattern of spread for b-ALS and l-ALS. B-ALS was characterized through GM changes in extra-motoric frontal and temporal regions, whilst only the l-ALS patients showed further cortical and subcortical changes within the PMC along with the transition towards disease Phase II (Fig. 3). A higher bulbar symptom burden (lower bulbar ALSFRS-R subscore) was associated with right-temporal and inferio-frontal GM density decreases as well as FA decreases in inter-hemispheric and long association tracts (Fig. 4).

Bulbar onset of symptoms in ALS is known to be a risk factor for shorter survival time and complications along with the disease course, as revealed in epidemiological cohort analyses (Calvo et al., 2017;

Ganesalingam et al., 2009; Trojsi et al., 2017). With means of VBM, the direct comparison between b-ALS and l-ALS showed more severe density decreases in many GM areas of all cerebral lobes and upper hemispheres of the cerebellum. This in principle coincides with regions that have been described in other VBM analyses before for cognitively normal b-ALS patients (Bede et al., 2013; Kim et al., 2017). Other neuroimaging studies (e.g. measuring cortical thinning) per se also suggested that b-ALS patients are specifically characterized by an early and widespread involvement of cerebral GM (Schuster et al., 2013; van der Burgh et al., 2020). In our study, especially cortical regions of the frontal and temporal lobes were widely affected and consistently corresponded with adjacent WM density decreases. Also for WM, some studies reported the affection of frontal and temporal pathways before for b-ALS in comparison to l-ALS (Hartung et al., 2014; Kim et al., 2017). Our study shows, that altogether the location of GM and WM changes did highly correspond and were not remarkably different between l-ALS and b-ALS in comparison to healthy controls. However, we observed more pronounced GM and WM atrophy in b-ALS in comparison to l-ALS in motor and extra-motor regions.

Noteworthy, most parts of the upper limb and trunk segments of the homunculus were spared in the PMC for the GM contrasts, whereas the segments related to the tongue and face were particularly involved in b-ALS patients. It was described before in region of interest (ROI) based studies, that a selective vulnerability of the orofacial motor-cortex segments is detectable for b-ALS (Bede et al., 2013; Jin et al., 2019; Schuster et al., 2013). However, we were able to demonstrate this selective vulnerability of the PMC in b-ALS using a whole-brain-based approach. Consequently, a possible explanation for the more severe affection of extra-motor GM and WM regions for b-ALS may arise from the theory of corticofugal spread of ALS-related neuropathology, originating from the PMC (Braak et al., 2013; Eisen et al., 2017). In conclusion, in b-ALS patients a pronounced and early spread of ALS pathology, especially to frontal GM and WM regions, could be caused by the naturally higher grade of cortico-cortical integration of the orofacial motor-cortex regions. Such projections are considered to functionally influence complex motor-performances of orofacial muscles, such as facial expressions or speech production (Greenlee et al., 2004; Morecraft et al., 2004; Tokuno et al., 1997). An increased vulnerability of the orofacial PMC, due to its high level of integration as neocortical structure, has been discussed in the context of ALS pathophysiology before (Devine et al., 2013; Eisen, 2009).

The notion that b-ALS is characterized by an earlier cortical and subcortical spread of pathology is further corroborated by our pseudo-longitudinal comparisons that suggest that this is a matter of the early disease Phase I and/or may occur within pre-symptomatic Phases of b-ALS. No expansion of further cortical involvement within the PMC has been observed in b-ALS along with the transition towards disease Phase II. On the contrary, l-ALS patients in Phase II have been characterized by significantly more density decreases in facial and upper limb parts of the PMC and adjacent WM. These effects have been more pronounced for the left hemisphere, which suggests a mirroring spread of pathology towards the primarily less affected side. In all contrasts of this study,
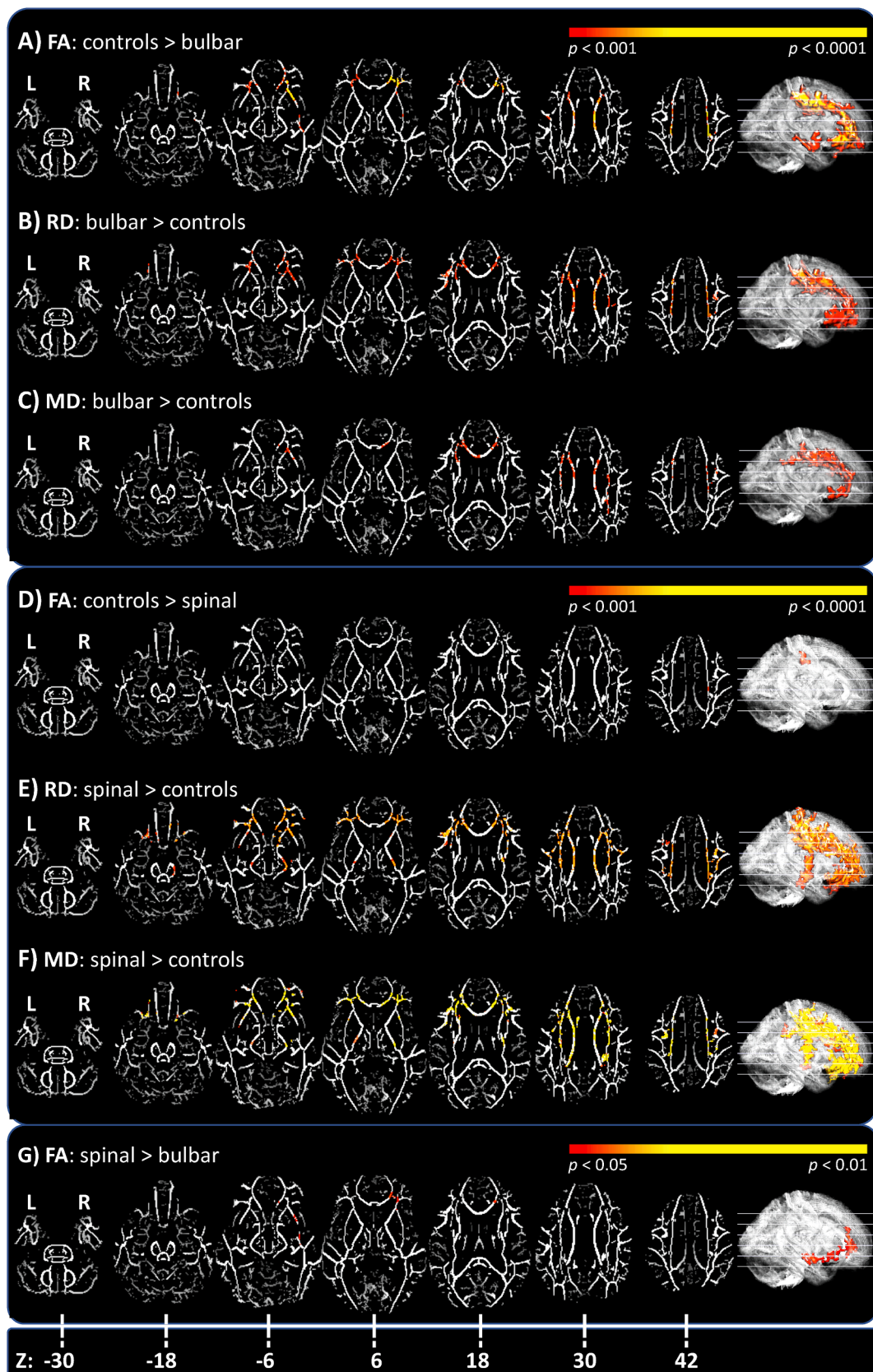
*(caption on next page)*

**Fig. 2.** TBSS group analyses of bulbar versus limb-onset ALS. The pictures show significant *p*-thresholded contrasts of TBSS inter-group comparisons for FA, AD, MD or RD respectively (red-yellow colorbar) overlaid on the averaged FA skeleton in representative axial slices (visualization with MRIcroGL). A-C) B-ALS vs. healthy controls: Revealed widespread FA decreases of b-ALS, most evident in the corpus callosum and adjacent corono radiata as well as long association tracts of frontal, parietal and temporal lobes. Increased RD was mainly co-localized with the decreased FA, whilst MD increases were more restricted. (TFCE; FWE corrected *p* < 0.001; nuisance co-variates: age, gender). D-F) B-ALS vs. healthy controls: The most significant changes were observed for increased MD, localized mainly in bifrontal WM including both CSTs, in some parts with overlapping RD increases. The FA contrast did only show a small cluster of decreased FA right subcortical of the precentral gyrus. (TFCE; FWE corrected *p* < 0.001; nuisance co-variates: age, gender). G) B-ALS vs. l-ALS: Showed only significant changes for FA. These decreases were located within the right-hemispehric WM, mainly the occipito-frontal fasciculus and the Forceps Minor. (TFCE; FWE corrected *p* < 0.05; nuisance co-variates: age, gender). *Abbreviations: AD:* Axial Diffusivity; *b-ALS:* bulbar-onset ALS; *CST:* Cortico-Spinal-Tract; *FA:* Fractional Anisotropy; *FWE:* Family-Wise Error; *l-ALS:* limb-onset ALS; *MD:* Mean Diffusivity; *RD:* Radial Diffusivity; *TFCE:* Threshold-Free Cluster Enhancement; *WM:* White Matter. (For interpretation of the references to colour in this figure legend, the reader is referred to the web version of this article.)

changes within the right hemisphere had been more evident, suggesting this the preferential side of pathology for this study cohort.

The TBSS analyses showed also ALS-related structural changes within known core regions of ALS pathology corresponding to the WM atrophy observed in the VBM analyses. Only the FA contrast showed differences in the direct subgroup comparisons between b-ALS and l-ALS, localized within right-frontal long association fiber tracts, mainly the occipito-frontal fasciculus. Former studies of both ALS onset-types, also described a dominance of FA changes for b-ALS (Borsodi et al., 2017; Cardenas-Blanco et al., 2014; Prell et al., 2013; van der Graaff et al., 2011). However, an advantage of the results described here is that we were consistently able to confirm the observations of case-control comparisons in direct subgroup analyses of b-ALS versus l-ALS. The FA changes evident in our b-ALS cohort underline the notion of an earlier and more severe affection of extra-motoric domains for this onset-type. This could be observed between b-ALS and l-ALS, despite equal disease Phases and aggressiveness of both subgroups. As such, these findings might indeed represent a neuroimaging correlate of a higher degree of cerebral pathology for b-ALS. Meanwhile, the l-ALS cohort is more represented by MD and RD changes, that are typically considered as a result of myelin changes (Song et al., 2002) and could be implicitly revealed within bilateral CSTs. The pseudo-longitudinal TBSS contrasts did not reveal any further changes in-between disease Phases I and II, which has been observed before (Steinbach et al., 2021). It could thus be suggested that changes within the major Fiber bundles, that are detectable with TBSS, are relatively stable in the ongoing disease, whilst the WM changes observed via VBM are possibly a correlate of extra-neuronal (e.g. glial) changes and/or affecting more diverse WM parts (e.g. subcortical). However, subtle changes may have been obfuscated due the usage of DTI sequences from a scanner with a relatively lower field strength (1.5 T) and only 30 diffusion directions applied. The MRIs used for this study were acquired on a scanner used in clinical routines, thus our results may have direct implications for diagnostic workups of patients, e.g. for regular stagings. Nevertheless, further studies using our approaches with 3 Tesla (or higher field strength) MRI data are necessary.

The regression analyses also confirmed the association between a higher bulbar dysfunction and a higher degree of impaired structural integrity, as significant correlations with the bulbar subscore could be revealed (which underlines the consistency of our results again). With means of VBM, higher bulbar burden was associated with more GM density decreases, again concentrated within frontal and right-temporal regions. To the best of our knowledge a similar correlation was not reported before, but Kim et al. showed correlations with the total ALSFRS-R almost solely for their b-ALS group, including bilateral frontal, left superior, and supramarginal gyri (Kim et al., 2017). We assume this could be driven by the lower bulbar subscore in this group. However, in our cohort the total ALSFRS-R did not correlate with VBM measures applying the same strict significance level. Notably, no significant regression results could be shown for any WM VBM contrast, neither with the total nor with any ALSFRS-R subscore, homologous former VBM studies that also failed to reveal direct associations with the total ALSFRS-R-score (Agosta et al., 2007; Kassubek et al., 2005; Rajagopalan and Pioro, 2014; Turner et al., 2007).

However, with means of TBSS widespread correlations could be shown, likewise former studies for the total ALSFRS-R (Cirillo et al., 2012; de Albuquerque et al., 2017; Prudlo et al., 2012; Sage et al., 2009; Trojsi et al., 2015). Here, our results again underline the notion that associations of scalar DTI values with the total ALSFRS-R score mostly rely on the degree of bulbar dysfunction, as co-localized patterns of associations have been revealed for both the total ALSFRS-R and the bulbar subscore. Thereby, the latter was most prominently reflected by widespread FA decreases, thus confirming our former subgroup analyses. Relations between the bulbar subscore and WM-DTI-changes have to the best of our knowledge not been described before. But Shellikeri et al. (2019) found associations of the speech dysdiadochokinese rate with FA and RD in orofacial parts of the right PMC. Also Roccatagliata et al. (2009) found reduced FA in the CST that correlated with a bulbar-burden-score.

In summary, our results indicate that b-ALS is mainly characterized by an early and widespread cortical pathology, implicitly affecting and probably originating from the orofacial segments of the PMC. With the ongoing disease until disease Phase II, further loss of structural integrity occurs in extra-motor-domains, mainly within the frontal and temporal lobes. Thus, b-ALS patients with the same degree of disease covered and equal aggressiveness profiles show more structural frontotemporal changes in comparison to l-ALS patients. In contrast, l-ALS shows worsening of GM as well as WM pathology within primary motor-regions along with the transition towards disease Phase II. This suggests that l-ALS patients have fewer cerebral structural integrity loss within the early course of the ALS disease, possibly due to a lower degree of neuronal network integration of the first pathologically affected regions.

This study is not free of limitations. First of all, it represents mono-centric data that cannot be generalized for all ALS patients. Moreover, a typical referral bias to tertiary ALS centers is known, where the ALS patients are more likely younger with a longer survival time and a smaller proportion of bulbar-onset, if compared to the geographical ALS population (Logroscino et al., 2018; Sorenson et al., 2007). Here, our b-ALS cohort had a significantly higher proportion of female patients (than in the l-ALS group), who were also older at symptom onset, which was reported from other studies of European ALS cohorts before (Calvo et al., 2017; Kim et al., 2017). Also, the conducted selection of patients with at least two ALSFRS-R assessments may have led to the exclusion of patients with rather higher disease aggressiveness, who were thus more likely lost to follow-up. Encompassing genetic profiles were also not available for the current ALS cohort, but would be desirable to search for potential associations of our neuroimaging finding with for example presence of C9orf72 expansions. Although we applied neurocognitive screening assessments to exclude patients with cognitive performances below normal range, we cannot exclude minor impairment for the patients with ALS. Further studies are needed, in cohorts that underwent consistent and thorough neurocognitive testing, including healthy controls. The subgroups of b-ALS and l-ALS had differing age and gender distributions; thus, all conducted analyses were accordingly corrected for these co-variates. Nevertheless, we propose that studying larger cohorts would be necessary to conduct additional analyses with e.g. pairwise matched patients to fully explore the potentially interacting
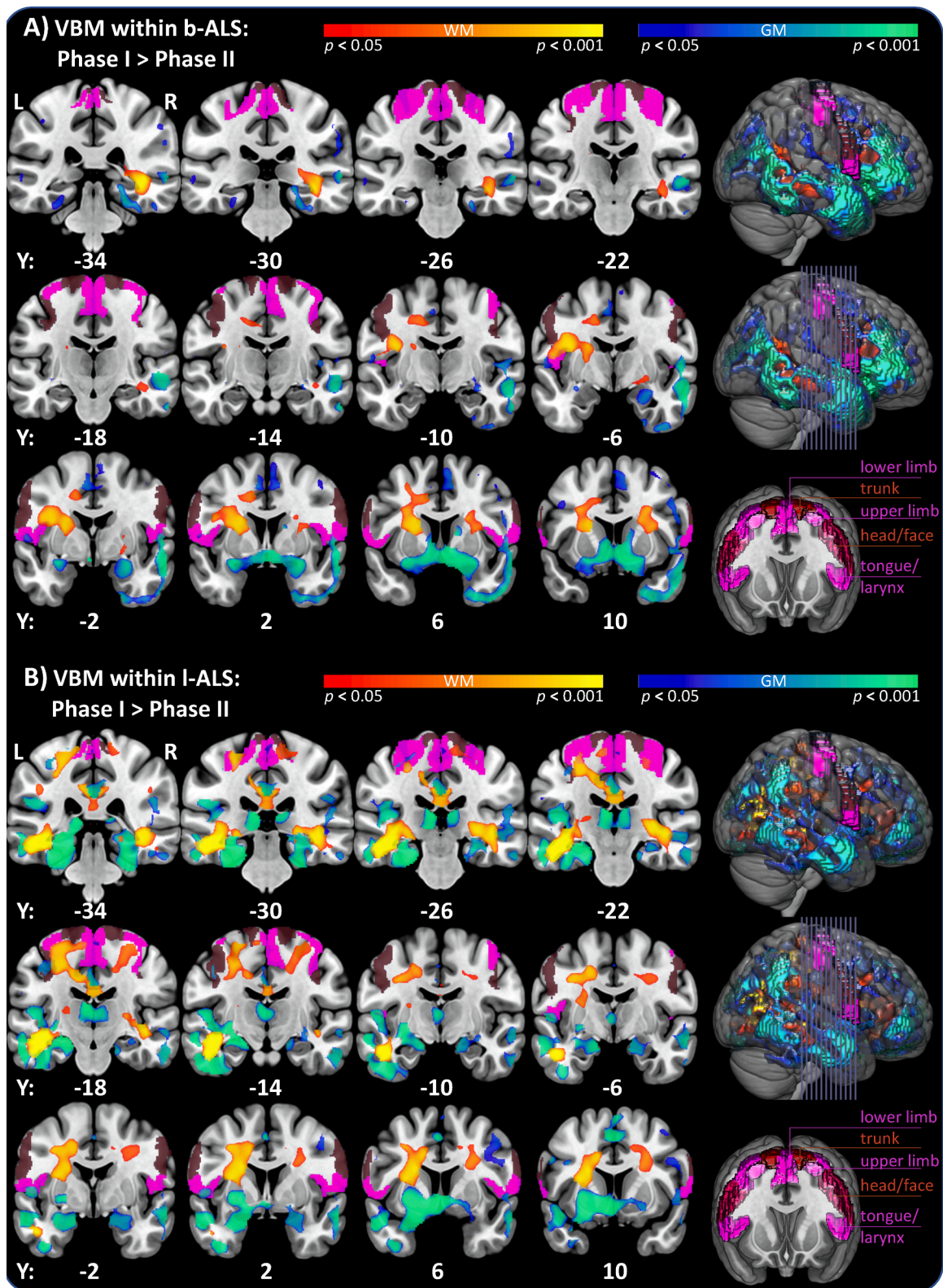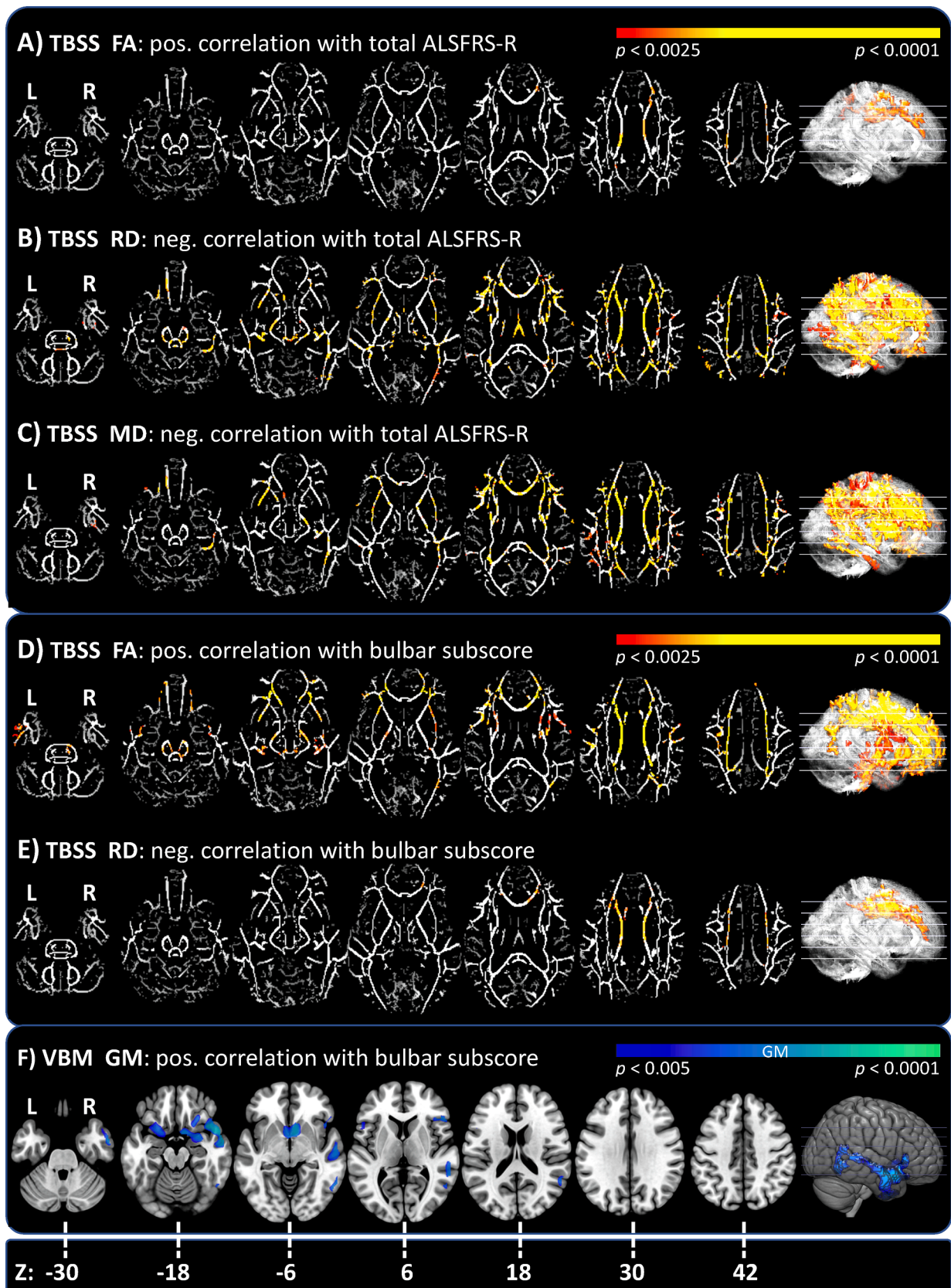
**Fig. 3.** Pseudolongitudinal comparison of b-ALS/l-ALS patients in Phase I versus II. The pictures show *p*-thresholded contrasts of VBM inter-group comparisons of GM (blue-green colorbar) and WM (red-yellow colorbar) overlaid on the MNI152_2009 template of MRIcroGL. Additionally, regions of the motopopic organization of the PMC have been overlaid (derived from the Brainnetome Atlas, violet and brown colors). A) Phase I vs. Phase II for b-ALS patients: GM and WM density decreases were revealed in bilateral temporal and inferio-frontal lobes, whilst no relevant additional changes have been revealed in the PMC. (TFCE; FWE corrected *p* < 0.05; nuisance co-variates: age, gender, TIV). B) Phase I vs. Phase II for l-ALS patients: The frontal and temporal GM/WM density decreases presented less extensive than the changes observed for b-ALS patients. Here, relevant changes within the PMC were revealed, localized mainly in the left hemispheric motoric areas representing the upper limbs. *Abbreviations: ALS:* Amyotrophic Lateral Sclerosis; *b-ALS:* bulbar-onset ALS; *FWE:* Family-Wise Error; *GM:* Grey Matter; *l-ALS:* limb-onset ALS; *PMC:* Primary Motor Cortex; *TFCE:* Threshold-Free Cluster Enhancement; *TIV:* Total Intracranial Volume; *WM:* White Matter. (For interpretation of the references to colour in this figure legend, the reader is referred to the web version of this article.)

A) TBSS FA: pos. correlation with total ALSFRS-R
B) TBSS RD: neg. correlation with total ALSFRS-R
C) TBSS MD: neg. correlation with total ALSFRS-R
D) TBSS FA: pos. correlation with bulbar subscore
E) TBSS RD: neg. correlation with bulbar subscore
F) VBM GM: pos. correlation with bulbar subscore

$p < 0.0025$   $p < 0.0001$

GM

$p < 0.005$   $p < 0.0001$

Z: -30   -18   -6   6   18   30   42

*(caption on next page)*

**Fig. 4.** Regression analyses with ALSFRS-R total score and bulbar subscore. The pictures show significant *p*-thresholded contrasts of regressions analyses. For TBSS analyses, FA, AD, MD or RD contrasts (red-yellow colorbar) are overlaid on the averaged FA skeleton and for the VBM GM contrast (blue-green colorbar) overlaid on the MNI152_2009 template, all showing the same representative axial slices (visualization with MRIcroGL). A significance threshold of $p < 0.05$ was accepted, the respective Bonferroni-adjusted *p*-values are given to account for multiple comparisons. A-C) TBSS correlations with ALSFRS-R: Widespread negative correlations for RD and mainly co-localized for MD have been found. Positive correlations with the FA have been more restricted, localized in the body of the corpus callosum and adjacent corona radiata. (TFCE; FWE corrected; $p < 0.0025$). D-F) TBSS correlations with the bulbar subscore: A positive correlation with FA was found for the entire corpus callosum with corona radiata and in addition long association tracts as well as the CSTs. Negative correlations with the RD were restricted to body and genu of the Corpus callosum. (TFCE; FWE corrected; $p < 0.0025$). G) VBM correlations with the bulbar subscore: A positive correlation was revealed, indicating density decreases that were associated with increased bulbar symptom burden. These were again localized in the inferior frontal gyrus and in the right temporal lobe. (TFCE; FWE corrected; $p < 0.005$; nuisance co-variates: TIV). *Abbreviations: AD:* Axial Diffusivity; *b-ALS:* bulbar-onset ALS; *CST:* Cortico-Spinal-Tract; *FA:* Fractional Anisotropy; *FWE:* Family-Wise Error; *l-ALS:* limb-onset ALS; *MD:* Mean Diffusivity; *RD:* Radial Diffusivity; *TFCE:* Threshold-Free Cluster Enhancement; *TIV:* Total Intracranial Volume; *WM:* White Matter. (For interpretation of the references to colour in this figure legend, the reader is referred to the web version of this article.)

effects of participants' demographics.

## 5. Conclusions

Our results show a higher degree of neurodegenerative burden in b-ALS that likely contributes to the known worse morbidity for this phenotypic subgroup of the ALS disease. This underlines the necessity of highly frequent advanced care planning of these patients in order to avoid early complications and to provide timely individualized therapy.

We provide strong rationales to separate or correct for the type of disease onset in ALS studies, whilst also considering the Phase of individual disease covered and disease aggressiveness profiles.

Future, large-scale and probably multi-center studies are needed to incorporate more aspects of phenotypic presentation, such as laterality, patterns of regional spread or genetic heterogeneity. We recommend using the D50 model in order to provide quantification and comparability of patients' highly individualized disease course.

## CRediT authorship contribution statement

**Robert Steinbach:** Conceptualization, Methodology, Software, Formal analysis, Investigation, Writing - original draft, Visualization, Writing - review & editing. **Tino Prell:** Formal analysis, Writing - review & editing. **Nayana Gaur:** Data curation, Writing - review & editing. **Annekathrin Roediger:** Investigation, Writing - review & editing. **Christian Gaser:** Methodology, Writing - review & editing. **Thomas E. Mayer:** Investigation, Resources, Writing - review & editing. **Otto W. Witte:** Funding acquisition, Writing - review & editing. **Julian Grosskreutz:** Conceptualization, Methodology, Formal analysis, Investigation, Resources, Data curation, Supervision, Project administration, Funding acquisition, Writing - review & editing.

## Declaration of Competing Interest

The authors declare that they have no known competing financial interests or personal relationships that could have appeared to influence the work reported in this paper.

## Appendix A. Supplementary data

Supplementary data to this article can be found online at https://doi.org/10.1016/j.nicl.2021.102674.

## References

Abrahams, S., Newton, J., Niven, E., Foley, J., Bak, T.H., 2014. Screening for cognition and behaviour changes in ALS. Amyotroph Lateral Scler Frontotemporal Degener 15, 9–14.

Agosta, F., Pagani, E., Rocca, M.A., Caputo, D., Perini, M., Salvi, F., Prelle, A., Filippi, M., 2007. Voxel-based morphometry study of brain volumetry and diffusivity in amyotrophic lateral sclerosis patients with mild disability. Hum Brain Mapp 28, 1430–1438.

Alruwaili, A.R., Pannek, K., Coulthard, A., Henderson, R., Kurniawan, N.D., McCombe, P., 2018. A combined tract-based spatial statistics and voxel-based morphometry study of the first MRI scan after diagnosis of amyotrophic lateral sclerosis with subgroup analysis. J Neuroradiol 45, 41–48.

Appollonio, I., Leone, M., Isella, V., Piamarta, F., Consoli, T., Villa, M.L., Forapani, E., Russo, A., Nichelli, P., 2005. The Frontal Assessment Battery (FAB): normative values in an Italian population sample. Neurol Sci 26, 108–116.

Bede, P., Bokde, A., Elamin, M., Byrne, S., McLaughlin, R.L., Jordan, N., Hampel, H., Gallagher, L., Lynch, C., Fagan, A.J., Pender, N., Hardiman, O., 2013. Grey matter correlates of clinical variables in amyotrophic lateral sclerosis (ALS): a neuroimaging study of ALS motor phenotype heterogeneity and cortical focality. J Neurol Neurosurg Psychiatry 84, 766–773.

Borsodi, F., Culea, V., Langkammer, C., Khalil, M., Pirpamer, L., Quasthoff, S., Enzinger, C., Schmidt, R., Fazekas, F., Ropele, S., 2017. Multimodal assessment of white matter tracts in amyotrophic lateral sclerosis. PloS one 12, e0178371.

Braak, H., Brettschneider, J., Ludolph, A.C., Lee, V.M., Trojanowski, J.Q., Del Tredici, K., 2013. Amyotrophic lateral sclerosis–a model of corticofugal axonal spread. Nat Rev Neurol 9, 708–714.

Brooks, B.R., Miller, R.G., Swash, M., Munsat, T.L., of on Diseases, W., 2000. El Escorial revisited: revised criteria for the diagnosis of amyotrophic lateral sclerosis. Amyotrophic lateral sclerosis and other motor neuron disorders : official publication of the World Federation of Neurology, Research Group on Motor Neuron Diseases 1, 293-299.

Calvo, A., Moglia, C., Lunetta, C., Marinou, K., Ticozzi, N., Ferrante, G.D., Scialo, C., Soraru, G., Trojsi, F., Conte, A., Falzone, Y.M., Tortelli, R., Russo, M., Chio, A., Sansone, V.A., Mora, G., Silani, V., Volanti, P., Caponnetto, C., Querin, G., Monsurro, M.R., Sabatelli, M., Riva, N., Logroscino, G., Messina, S., Fini, N., Mandrioli, J., 2017. Factors predicting survival in ALS: a multicenter Italian study. J Neurol 264, 54–63.

Cardenas-Blanco, A., Machts, J., Acosta-Cabronero, J., Kaufmann, J., Abdulla, S., Kollewe, K., Petri, S., Heinze, H.J., Dengler, R., Vielhaber, S., Nestor, P.J., 2014. Central white matter degeneration in bulbar- and limb-onset amyotrophic lateral sclerosis. J Neurol 261, 1961–1967.

Cedarbaum, J.M., Stambler, N., Malta, E., Fuller, C., Hilt, D., Thurmond, B., Nakanishi, A., 1999. The ALSFRS-R: a revised ALS functional rating scale that incorporates assessments of respiratory function. BDNF ALS Study Group (Phase III). J Neurol Sci 169, 13–21.

Chio, A., Hammond, E.R., Mora, G., Bonito, V., Filippini, G., 2015. Development and evaluation of a clinical staging system for amyotrophic lateral sclerosis. J Neurol Neurosurg Psychiatry 86, 38–44.

Cirillo, M., Esposito, F., Tedeschi, G., Caiazzo, G., Sagnelli, A., Piccirillo, G., Conforti, R., Tortora, F., Monsurro, M.R., Cirillo, S., Trojsi, F., 2012. Widespread microstructural

white matter involvement in amyotrophic lateral sclerosis: a whole-brain DTI study. AJNR Am J Neuroradiol 33, 1102–1108.

Creavin, S.T., Wisniewski, S., Noel-Storr, A.H., Trevelyan, C.M., Hampton, T., Rayment, D., Thom, V.M., Nash, K.J., Elhamoui, H., Milligan, R., Patel, A.S., Tsivos, D.V., Wing, T., Phillips, E., Kellman, S.M., Shackleton, H.L., Singleton, G.F., Neale, B.E., Watton, M.E., Cullum, S., 2016. Mini-Mental State Examination (MMSE) for the detection of dementia in clinically unevaluated people aged 65 and over in community and primary care populations. Cochrane Database Syst Rev, CD011145.

de Albuquerque, M., Branco, L.M., Rezende, T.J., de Andrade, H.M., Nucci, A., Franca Jr., M.C., 2017. Longitudinal evaluation of cerebral and spinal cord damage in Amyotrophic Lateral Sclerosis. Neuroimage Clin 14, 269–276.

Devine, M.S., Farrell, A., Woodhouse, H., McCombe, P.A., Henderson, R.D., 2013. A developmental perspective on bulbar involvement in amyotrophic lateral sclerosis. Amyotroph Lateral Scler Frontotemporal Degener 14, 638–639.

Dubois, B., Slachevsky, A., Litvan, I., Pillon, B., 2000. The FAB: a Frontal Assessment Battery at bedside. Neurology 55, 1621–1626.

Eisen, A., 2009. Amyotrophic lateral sclerosis-Evolutionary and other perspectives. Muscle Nerve 40, 297–304.

Eisen, A., Braak, H., Del Tredici, K., Lemon, R., Ludolph, A.C., Kiernan, M.C., 2017. Cortical influences drive amyotrophic lateral sclerosis. J Neurol Neurosurg Psychiatry 88, 917–924.

Fan, L., Li, H., Zhuo, J., Zhang, Y., Wang, J., Chen, L., Yang, Z., Chu, C., Xie, S., Laird, A. R., Fox, P.T., Eickhoff, S.B., Yu, C., Jiang, T., 2016. The Human Brainnetome Atlas: A New Brain Atlas Based on Connectional Architecture. Cereb Cortex 26, 3508–3526.

Floeter, M.K., Danielian, L.E., Braun, L.E., Wu, T., 2018. Longitudinal diffusion imaging across the C9orf72 clinical spectrum. J Neurol Neurosurg Psychiatry 89, 53–60.

Ganesalingam, J., Stahl, D., Wijesekera, L., Galtrey, C., Shaw, C.E., Leigh, P.N., Al-Chalabi, A., 2009. Latent cluster analysis of ALS phenotypes identifies prognostically differing groups. PloS one 4, e7107.

Genon, S., Reid, A., Li, H., Fan, L., Muller, V.I., Cieslik, E.C., Hoffstaedter, F., Langner, R., Grefkes, C., Laird, A.R., Fox, P.T., Jiang, T., Amunts, K., Eickhoff, S.B., 2018. The heterogeneity of the left dorsal premotor cortex evidenced by multimodal connectivity-based parcellation and functional characterization. Neuroimage 170, 400–411.

Greenlee, J.D., Oya, H., Kawasaki, H., Volkov, I.O., Kaufman, O.P., Kovach, C., Howard, M.A., Brugge, J.F., 2004. A functional connection between inferior frontal gyrus and orofacial motor cortex in human. J Neurophysiol 92, 1153–1164.

Hartung, V., Prell, T., Gaser, C., Turner, M.R., Tietz, F., Ilse, B., Bokemeyer, M., Witte, O. W., Grosskreutz, J., 2014. Voxel-based MRI intensitometry reveals extent of cerebral white matter pathology in amyotrophic lateral sclerosis. PloS one 9, e104894.

Jin, J., Hu, F., Zhang, Q., Chen, Q., Li, H., Qin, X., Jia, R., Kang, L., Dang, Y., Dang, J., 2019. Dominant Heterogeneity of Upper and Lower Motor Neuron Degeneration to Motor Manifestation of Involved Region in Amyotrophic Lateral Sclerosis. Sci Rep 9, 20059.

Kassubek, J., Unrath, A., Huppertz, H.J., Lule, D., Ethofer, T., Sperfeld, A.D., Ludolph, A. C., 2005. Global brain atrophy and corticospinal tract alterations in ALS, as investigated by voxel-based morphometry of 3-D MRI. Amyotroph Lateral Scler Other Motor Neuron Disord 6, 213–220.

Kim, H.J., de Leon, M., Wang, X., Kim, H.Y., Lee, Y.J., Kim, Y.H., Kim, S.H., 2017. Relationship between Clinical Parameters and Brain Structure in Sporadic Amyotrophic Lateral Sclerosis Patients According to Onset Type: A Voxel-Based Morphometric Study. PloS one 12, e0168424.

Logroscino, G., Marin, B., Piccininni, M., Arcuti, S., Chio, A., Hardiman, O., Rooney, J., Zoccolella, S., Couratier, P., Preux, P.M., Beghi, E., for, E, 2018. Referral bias in ALS epidemiological studies. PloS one 13, e0195821.

Lule, D., Burkhardt, C., Abdulla, S., Bohm, S., Kollewe, K., Uttner, I., Abrahams, S., Bak, T.H., Petri, S., Weber, M., Ludolph, A.C., 2015. The Edinburgh Cognitive and Behavioural Amyotrophic Lateral Sclerosis Screen: a cross-sectional comparison of established screening tools in a German-Swiss population. Amyotroph Lateral Scler Frontotemporal Degener 16, 16–23.

Morecraft, R.J., Stilwell-Morecraft, K.S., Rossing, W.R., 2004. The motor cortex and facial expression: new insights from neuroscience. Neurologist 10, 235–249.

Poesen, K., De Schaepdryver, M., Stubendorff, B., Gille, B., Muckova, P., Wendler, S., Prell, T., Ringer, T.M., Rhode, H., Stevens, O., Claeys, K.G., Couwelier, G., D'Hondt, A., Lamaire, N., Tilkin, P., Van Reijen, D., Gourmaud, S., Fedtke, N., Heiling, B., Rumpel, M., Rodiger, A., Gunkel, A., Witte, O.W., Paquet, C., Vandenberghe, R., Grosskreutz, J., Van Damme, P., 2017. Neurofilament markers for ALS correlate with extent of upper and lower motor neuron disease. Neurology 88, 2302–2309.

Prell, T., Gaur, N., Steinbach, R., Witte, O.W., Grosskreutz, J., 2020. Modelling disease course in amyotrophic lateral sclerosis: pseudo-longitudinal insights from cross-sectional health-related quality of life data. Health Qual Life Outcomes 18, 117.

Prell, T., Peschel, T., Hartung, V., Kaufmann, J., Klauschies, R., Bodammer, N., Kollewe, K., Dengler, R., Grosskreutz, J., 2013. Diffusion tensor imaging patterns differ in bulbar and limb onset amyotrophic lateral sclerosis. Clin Neurol Neurosurg 115, 1281–1287.

Prudlo, J., Bissbort, C., Glass, A., Grossmann, A., Hauenstein, K., Benecke, R., Teipel, S.J., 2012. White matter pathology in ALS and lower motor neuron ALS variants: a diffusion tensor imaging study using tract-based spatial statistics. J Neurol 259, 1848–1859.

Rajagopalan, V., Pioro, E.P., 2014. Distinct patterns of cortical atrophy in ALS patients with or without dementia: an MRI VBM study. Amyotroph Lateral Scler Frontotemporal Degener 15, 216–225.

Roccatagliata, L., Bonzano, L., Mancardi, G., Canepa, C., Caponnetto, C., 2009. Detection of motor cortex thinning and corticospinal tract involvement by quantitative MRI in amyotrophic lateral sclerosis. Amyotroph Lateral Scler 10, 47–52.

Roche, J.C., Rojas-Garcia, R., Scott, K.M., Scotton, W., Ellis, C.E., Burman, R., Wijesekera, L., Turner, M.R., Leigh, P.N., Shaw, C.E., Al-Chalabi, A., 2012. A proposed staging system for amyotrophic lateral sclerosis. Brain 135, 847–852.

Sage, C.A., Van Hecke, W., Peeters, R., Sijbers, J., Robberecht, W., Parizel, P., Marchal, G., Leemans, A., Sunaert, S., 2009. Quantitative diffusion tensor imaging in amyotrophic lateral sclerosis: revisited. Hum Brain Mapp 30, 3657–3675.

Schuster, C., Kasper, E., Machts, J., Bittner, D., Kaufmann, J., Benecke, R., Teipel, S., Vielhaber, S., Prudlo, J., 2013. Focal thinning of the motor cortex mirrors clinical features of amyotrophic lateral sclerosis and their phenotypes: a neuroimaging study. J Neurol 260, 2856–2864.

Shellikeri, S., Myers, M., Black, S.E., Abrahao, A., Zinman, L., Yunusova, Y., 2019. Speech network regional involvement in bulbar ALS: a multimodal structural MRI study. Amyotroph Lateral Scler Frontotemporal Degener 20, 385–395.

Simon, N.G., Turner, M.R., Vucic, S., Al-Chalabi, A., Shefner, J., Lomen-Hoerth, C., Kiernan, M.C., 2014. Quantifying disease progression in amyotrophic lateral sclerosis. Ann Neurol 76, 643–657.

Smith, S.M., Nichols, T.E., 2009. Threshold-free cluster enhancement: addressing problems of smoothing, threshold dependence and localisation in cluster inference. Neuroimage 44, 83–98.

Song, S.K., Sun, S.W., Ramsbottom, M.J., Chang, C., Russell, J., Cross, A.H., 2002. Dysmyelination revealed through MRI as increased radial (but unchanged axial) diffusion of water. Neuroimage 17, 1429–1436.

Sorenson, E.J., Mandrekar, J., Crum, B., Stevens, J.C., 2007. Effect of referral bias on assessing survival in ALS. Neurology 68, 600–602.

Steinbach, R., Batyrbekova, M., Gaur, N., Voss, A., Stubendorff, B., Mayer, T.E., Gaser, C., Witte, O.W., Prell, T., Grosskreutz, J., 2020a. Applying the D50 disease progression model to gray and white matter pathology in amyotrophic lateral sclerosis. Neuroimage Clin 25, 102094.

Steinbach, R., Gaur, N., Roediger, A., Mayer, T.E., Witte, O.W., Prell, T., Grosskreutz, J., 2021. Disease aggressiveness signatures of amyotrophic lateral sclerosis in white matter tracts revealed by the D50 disease progression model. Hum Brain Mapp 42, 737–752.

Steinbach, R., Prell, T., Gaur, N., Stubendorff, B., Roediger, A., Ilse, B., Witte, O.W., Grosskreutz, J., 2020b. Triage of Amyotrophic Lateral Sclerosis Patients during the COVID-19 Pandemic: An Application of the D50 Model. J Clin Med 9, 2873.

Tokuno, H., Takada, M., Nambu, A., Inase, M., 1997. Reevaluation of ipsilateral corticocortical inputs to the orofacial region of the primary motor cortex in the macaque monkey. J Comp Neurol 389, 34–48.

Trojsi, F., Caiazzo, G., Corbo, D., Piccirillo, G., Cristillo, V., Femiano, C., Ferrantino, T., Cirillo, M., Monsurro, M.R., Esposito, F., Tedeschi, G., 2015. Microstructural changes across different clinical milestones of disease in amyotrophic lateral sclerosis. PloS one 10, e0119045.

Trojsi, F., Siciliano, M., Femiano, C., Santangelo, G., Lunetta, C., Calvo, A., Moglia, C., Marinou, K., Ticozzi, N., Drago Ferrante, G., Scialo, C., Soraru, G., Conte, A., Falzone, Y.M., Tortelli, R., Russo, M., Sansone, V.A., Chio, A., Mora, G., Poletti, B., Volanti, P., Caponnetto, C., Querin, G., Sabatelli, M., Riva, N., Logroscino, G., Messina, S., Fasano, A., Monsurro, M.R., Tedeschi, G., Mandrioli, J., 2017. Comorbidity of dementia with amyotrophic lateral sclerosis (ALS): insights from a large multicenter Italian cohort. J Neurol 264, 2224–2231.

Turner, M.R., Hammers, A., Allsop, J., Al-Chalabi, A., Shaw, C.E., Brooks, D.J., Leigh, P. N., Andersen, P.M., 2007. Volumetric cortical loss in sporadic and familial amyotrophic lateral sclerosis. Amyotroph Lateral Scler 8, 343–347.

van der Burgh, H.K., Westeneng, H.J., Walhout, R., van Veenhuijzen, K., Tan, H.H.G., Meier, J.M., Bakker, L.A., Hendrikse, J., van Es, M.A., Veldink, J.H., van den Heuvel, M.P., van den Berg, L.H., 2020. Multimodal longitudinal study of structural brain involvement in amyotrophic lateral sclerosis. Neurology.

van der Graaff, M.M., Sage, C.A., Caan, M.W., Akkerman, E.M., Lavini, C., Majoie, C.B., Nederveen, A.J., Zwinderman, A.H., Vos, F., Brugman, F., van den Berg, L.H., de Rijk, M.C., van Doorn, P.A., Van Hecke, W., Peeters, R.R., Robberecht, W., Sunaert, S., de Visser, M., 2011. Upper and extra-motoneuron involvement in early motoneuron disease: a diffusion tensor imaging study. Brain 134, 1211–1228.

Verstraete, E., Turner, M.R., Grosskreutz, J., Filippi, M., Benatar, M., attendees of the 4th Ni, S.m., 2015. Mind the gap: the mismatch between clinical and imaging metrics in ALS. Amyotroph Lateral Scler Frontotemporal Degener 16, 524-529.

Westeneng, H.J., Debray, T.P.A., Visser, A.E., van Eijk, R.P.A., Rooney, J.P.K., Calvo, A., Martin, S., McDermott, C.J., Thompson, A.G., Pinto, S., Kobeleva, X., Rosenbohm, A., Stubendorff, B., Sommer, H., Middelkoop, B.M., Dekker, A.M., van Vugt, J., van Rheenen, W., Vajda, A., Heverin, M., Kazoka, M., Hollinger, H., Gromicho, M., Korner, S., Ringer, T.M., Rodiger, A., Gunkel, A., Shaw, C.E., Bredenoord, A.L., van Es, M.A., Corcia, P., Couratier, P., Weber, M., Grosskreutz, J., Ludolph, A.C., Petri, S., de Carvalho, M., Van Damme, P., Talbot, K., Turner, M.R., Shaw, P.J., Al-Chalabi, A., Chio, A., Hardiman, O., Moons, K.G.M., Veldink, J.H., van den Berg, L.H., 2018. Prognosis for patients with amyotrophic lateral sclerosis: development and validation of a personalised prediction model. Lancet Neurol 17, 423–433.

Winkler, A.M., Ridgway, G.R., Webster, M.A., Smith, S.M., Nichols, T.E., 2014. Permutation inference for the general linear model. Neuroimage 92, 381–397.

Zhang, F., Chen, G., He, M., Dai, J., Shang, H., Gong, Q., Jia, Z., 2018. Altered white matter microarchitecture in amyotrophic lateral sclerosis: a voxel-based meta-analysis of diffusion tensor imaging. Neuroimage Clin 19, 122–129.

Zhang, J., Ji, B., Hu, J., Zhou, C., Li, L., Li, Z., Huang, X., Hu, X., 2017. Aberrant interhemispheric homotopic functional and structural connectivity in amyotrophic lateral sclerosis. J Neurol Neurosurg Psychiatry 88, 369–370.